

# On the Use of the Center of Percussion for Space Manipulators during Impacts

Iosif S. Paraskevas, *Student Member, IEEE* and Evangelos G. Papadopoulos, *Senior Member, IEEE*

**Abstract**—One of the most demanding tasks for a robotic servicer is capturing a target. During this task, the mechanical systems can be subject to large forces for short duration (impacts). In space servicers, these impacts may render the capturing of a target impossible without the use of undesirable fuel-consuming maneuvers. This paper presents an approach for minimizing impact reactions, using the Center of Percussion (CoP), a characteristic of rigid bodies rotating around an axis. This work generalizes and delineates the exact requirements for its use. Application of CoP in multibody systems is demonstrated using the Newton-Euler Algorithm. Implementation guidelines are discussed. Simulations of a planar space robot system, and a three-dimensional PUMA-like manipulator on a satellite base confirm the benefit of using the CoP during tasks that include impacts.

## I. INTRODUCTION

The exploitation of space requires the establishment of both human and robotic presence. Towards this, various roadmaps indicate the need for the realization of a robotic orbital infrastructure for tasks such as satellite servicing, orbital debris removal and construction of large assemblies on Earth or other planetary orbits. To this end, On-Orbit Servicing (OOS) plays a central part.

A demanding task for OOS is capturing a target by a space robotic system, consisting of a satellite base and one or more manipulators mounted on it. Difficulties arise due to the dynamic coupling between the base and the manipulator, see for example [1]. Capturing is inevitably connected with impact forces as the chaser and the target come into contact. This task is more challenging when the robotic system and the target have comparable mass. In order to minimize the reaction forces, the reduction of impulse on the body using the Extended Inertia Tensor has been proposed [2], and the concept of virtual mass and the impedance matching of both systems were studied [3]. Notable works focus on the problem taking into account the system dynamics, mainly the post impact ones, e.g. [4].

This work proposes a method for minimizing negative reaction stresses on the chaser during impacts. It exploits the physical characteristics of any body capable of rotating around an axis. It is based on a property known in mechanics, called the Center of Percussion (CoP) or

Percussion Point. Its primary use is in sports equipment (e.g. tennis rackets, baseball bats) and hand tools (e.g. hammers). For example, if an external force acts on a bat's CoP, less stress is produced on the hands of a player (sweet spot), e.g. [5]. The CoP has been of limited use so far in other areas although some interesting works have been developed during the last decade. In [6], a novel method which exploits the CoP for legged locomotion is proposed, by considering the foot while in stance, as a pivot. Another work for bipeds uses the CoP for weight lifting [7]. In [8], the authors use the CoP to minimize the reactions on a wagon when it encounters an object. In [9], the existence of multiple CoPs at flexible beams is presented. Generally, the analytical description in the bibliography is scarce. An earlier version of this work, which presented preliminary ideas, is [10].

The motivation for exploiting the CoP for a robot, especially a space-borne one, is twofold. First, the use of the CoP is expected to reduce the reaction forces on its joint bearings, reducing the developed stresses and consequently the probability of mechanical failure. Secondly, especially for space systems, the reaction reduction minimizes the translational forces that affect the free-flier base, minimizing the tendency of the chaser to move away from the target after an impact (especially following an unsuccessful capture). Staying close to the target also minimizes the fuel that would be required to approach the target again.

This paper establishes the theoretical basis of CoP in Section II, and generalizes the concept in 3D in Section III. In Section IV, its use in multibody systems is shown using the Newton-Euler Approach (NEA). Implementation guidelines for various manipulator types are discussed in Section V. In Section VI, simulations of a planar space robot system, and a space robot with a 3R manipulator confirm the benefit of using the CoP during tasks that include impacts.

## II. 2D CENTER OF PERCUSSION ANALYSIS

*Assumptions.* The following assumptions apply [11]: (i) Impacts are between rigid bodies. The contact area remains small in comparison to other dimensions, (ii) Impact forces are very high and for short duration, therefore the impulse of forces like gravity is negligible. It is assumed that there is no considerable change at system configuration during an impact. This applies also in zero-g even if there is no fixed base, because each joint appears as fixed in a position during impact ("quasi-fixed"), and (iii) Relative velocities between bodies are within the limits of low speed impacts in order to avoid plastic yield. No requirement is set for the exact impact/contact model or the coefficient of restitution. The assumptions are valid also for the 3D and multibody cases. Manipulator workspace and singularity issues are out of the scope of this work.

---

\*This research has been co-financed by the European Union (European Social Fund – ESF) and Greek national funds through the Operational Program "Education and Lifelong Learning" of the National Strategic Reference Framework (NSRF) - Research Funding Program: Heracleitus II. Investing in knowledge society through the European Social Fund.

Iosif S. Paraskevas and Evangelos Papadopoulos are with the Dept. of Mechanical Eng., National Technical University of Athens, 9 Heroon Polytechniou str., 15780 Athens, Greece (e-mail: isparas@mail.ntua.gr; egpapado@central.ntua.gr; phone: +30-210-772-1440).

*The concept of CoP.* The CoP is a property of bodies able to rotate about a fixed axis. If an impact occurs at the CoP, the reaction force which is exerted on the fixed rotation axis (i.e. on the bearings of the rotational joint), tends to a minimum including zero. Let a beam, see Fig. 1, that can rotate about a Rotation Axis (RA). An impact occurs at a point on the longitudinal axis and the overall movement of the body consists of the superposition of (i) a translation in the direction of the impulse, therefore an inertial force is exerted at its RA and (ii) a rotation around its Center of Mass (CM), thus exerting an inertial force at the RA, at a direction opposite to that of the previous one (CM acts as a fulcrum). The vectorial sum of the forces exerted on the RA is the reaction force during the impact. If the impact occurs at the CoP, it will produce zero reaction force.

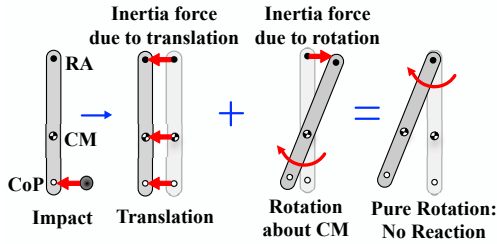


Figure 1. The concept of CoP: how the reaction forces can be zeroed.

To study this concept analytically, consider the free body diagram in Fig. 2. Assume an impact force at some point (impact point - IP) along the longitudinal axis. For purposes of generality, the impact force can have any direction. Balance of forces and moments yield,

$$-m \cdot \dot{v}_{cm} \cdot \sin\theta = -m \cdot \ddot{\theta} \cdot r_{cm} \cdot \sin\theta = N_x - F_{imp} \cdot \cos(\phi + \theta) \quad (1)$$

$$m \cdot \dot{v}_{cm} \cdot \cos\theta = m \cdot \ddot{\theta} \cdot r_{cm} \cdot \cos\theta = N_y - F_{imp} \cdot \sin(\phi + \theta) \quad (2)$$

$$I^o \cdot \ddot{\theta} = -l \cdot F_{imp} \cdot \sin\phi \quad (3)$$

where all symbols are defined in Fig. 2 and  $m$  is the mass of the body. The body polar inertia  $I^o$  around the RA at O is,

$$I^o = I^c + m \cdot r_{cm}^2 \quad (4)$$

where  $I^c$  is the body polar inertia with respect to the CM.

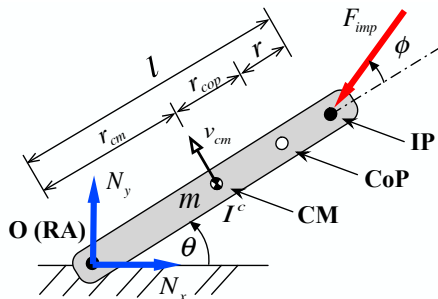


Figure 2. Free body diagram of a beam under impact force.

The impact point is located at distance

$$l = l_{cop} + r = (r_{cop} + r_{cm}) + r \quad (5)$$

from point O. Integrating (1) - (3) for a small fraction of time, transforms the forces into corresponding impulses (e.g.  $N_x \rightarrow \Omega_{Nx}$ ) and accelerations into velocities. Applying algebraic manipulation and trigonometric identities, the

magnitude of the impulse of the reaction force  $N$ ,  $\Omega_N$ , is given by,

$$\Omega_N^2 = \Omega_{Nx}^2 + \Omega_{Ny}^2 = \Omega_{F_{imp}}^2 \cdot \left[ 1 + (C_{ID}^2 - 2 \cdot C_{ID}) \cdot \sin^2 \phi \right] \quad (6)$$

with

$$C_{ID} = l \cdot r_{cm} \cdot m \cdot (I^o)^{-1} \quad (7)$$

where  $C_{ID}$  is the Coefficient of Impact Design, a term which relates the physical characteristics of the body to the location of the impact. Equations are simplified using the non-dimensional impulse

$$\tilde{\Omega}_N = \sqrt{\Omega_N^2 / \Omega_{F_{imp}}^2} \quad (8)$$

Equation (6) does not depend on the beam angle  $\theta$ , but it depends solely on the angle of impact  $\phi$  and the position of impact due to (7). In order to find the CoP, one can set

$$\tilde{\Omega}_N = 0 \Leftrightarrow \phi = \text{Arcsin} \left[ (2 \cdot C_{ID} - C_{ID}^2)^{-1/2} \right] = \text{Arcsin} \beta \quad (9)$$

The term  $\text{Arcsin}$  is valid for  $\beta \leq 1$ , while the radicand of the square root is valid only for  $0 < C_{ID} < 2$ , meaning that  $\beta \geq 1$ . Therefore, the reaction impulse will be eliminated if and only if

$$\tilde{\Omega}_N = 0 \Leftrightarrow \beta = 1 \Leftrightarrow \phi = \pm \pi/2 \quad \text{and} \quad C_{ID} = 1 \quad (10)$$

The sign defines the force direction. Equation (10) proves the uniqueness of the CoP along the longitudinal axis of a beam. From (7), and using (10) and (5) for  $r=0$  (impact occurs at the CoP), it can be found that the CoP's location is

$$r_{cop} = I^c \cdot (r_{cm} \cdot m)^{-1} \quad (11)$$

If  $r_{cm} \rightarrow 0 \Leftrightarrow r_{cop} \rightarrow +\infty$ , i.e. the reaction forces cannot be eliminated on a statically balanced body. If  $r_{cm} \rightarrow +\infty \Leftrightarrow r_{cop} \rightarrow 0$ , the CoP coincides with the CM.

*General impacts.* Next, we examine the sensitivity of  $\tilde{\Omega}_N$  when either the  $C_{ID}$  or the angle  $\phi$  change. Fig. 3a shows  $\partial(\tilde{\Omega}_N)/\partial\phi$  as a function of  $\phi$ . It can be seen that the sensitivity is highest when  $C_{ID} = 1$ . Similarly Fig. 3b shows  $\partial(\tilde{\Omega}_N)/\partial C_{ID}$  as a function of  $C_{ID}$ . We observe that the highest sensitivity is at  $\phi = 90^\circ$ . This sensitivity analysis showed that deviations from the normal impact angle yield higher rate of change of the reaction forces than deviations from the impact location of the CoP; yet the penalty is that at the non-CoP points the reaction forces can never be eliminated. The controller should try to achieve the requirements of the percussion point as in (10), and if this is not achievable it should try to keep the angle of the impact as close to  $\phi = 90^\circ$  as possible.

### III. CoP ANALYSIS IN 3D IMPACTS

We consider the rigid body of Fig. 4 whose Center of Rotation (CR) is located at the spherical joint O. Let a force

$\mathbf{F}_{imp}$  acting on it. The equations of motion for the Coordinate System (CS)  $a: \{xyz\}$  are

$$\sum {}^a \mathbf{F}_o = m \cdot {}^a \dot{\mathbf{v}}_{cm} = {}^a \mathbf{N} + {}^a \mathbf{F}_{imp} \quad (12)$$

$$\sum {}^a \mathbf{M}_o = d/dt ({}^a \mathbf{I}^o \cdot {}^a \boldsymbol{\omega}) = ({}^a \mathbf{l}_{imp} \times {}^a \mathbf{F}_{imp}) \quad (13)$$

where  $\mathbf{N}$  is the reaction force at O and  $\mathbf{I}^o$  is the inertia matrix of the body with respect to O. For any CS, the following holds ( $\mathbf{1}_3$  is the 3x3 unit matrix)

$$\mathbf{v}_{cm} = \boldsymbol{\omega} \times \mathbf{r}_{cm} \quad (14)$$

$$\mathbf{l}_{imp} = \mathbf{r}_{cm} + \mathbf{r}_{imp} = \mathbf{r}_{cm} + \mathbf{r}_{cop} + \mathbf{r} = \mathbf{l}_{cop} + \mathbf{r} \quad (15)$$

$$\mathbf{I}^o = \mathbf{I}^c + m \cdot (\mathbf{r}_{cm}^T \cdot \mathbf{r}_{cm} \cdot \mathbf{1}_3 - \mathbf{r}_{cm} \cdot \mathbf{r}_{cm}^T) \quad (16)$$

where  $\mathbf{I}^c$  is the inertia matrix with respect to CM. Integrating for a short duration (12) and (13), using (14) and performing some algebraic manipulation we find that

$${}^a \mathbf{I}^o \cdot {}^a \boldsymbol{\omega} = [{}^a \mathbf{l}_{imp} \times (m \cdot {}^a \boldsymbol{\omega} \times {}^a \mathbf{r}_{cm} - {}^a \boldsymbol{\Omega}_N)] \quad (17)$$

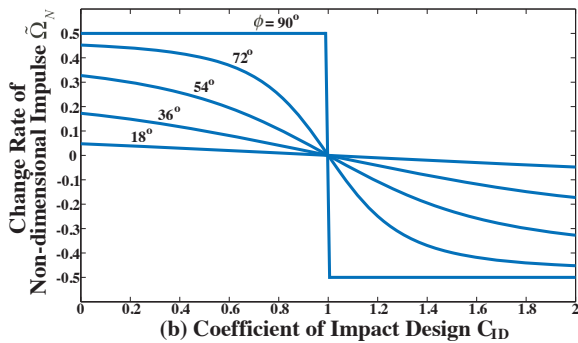
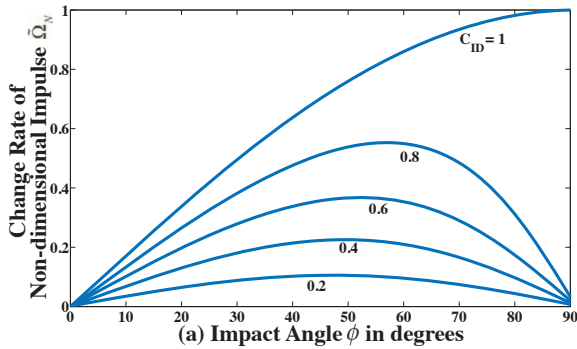


Figure 3. Change rate of non-dimensional impulse as (a) Impact angle changes and (b) as the coefficient of impact design changes.

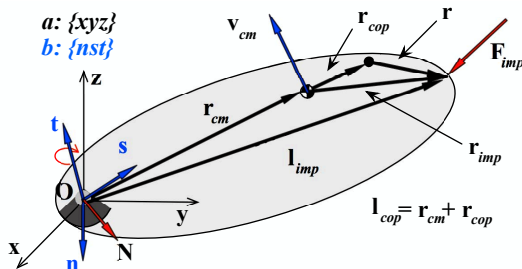


Figure 4. A 3D rigid body rotating around a spherical joint and the geometrical elements used to derive the CoP conditions in 3D case.

where  ${}^a \boldsymbol{\Omega}_N$  is the reaction impulse at point O, and can be considered as the vectorial sum of a normal,  $\boldsymbol{\Omega}_{N\perp}$ , and a parallel,  $\boldsymbol{\Omega}_{N\parallel}$ , component to the impact vector  $\mathbf{l}_{imp}$ :

$$\boldsymbol{\Omega}_N = \boldsymbol{\Omega}_{N\perp} + \boldsymbol{\Omega}_{N\parallel} \quad (18)$$

Using (18) in (17):

$${}^a \mathbf{I}^o \cdot {}^a \boldsymbol{\omega} - {}^a \mathbf{l}_{imp} \times (m \cdot {}^a \boldsymbol{\omega} \times {}^a \mathbf{r}_{cm}) = {}^a \boldsymbol{\Omega}_{N\perp} \times {}^a \mathbf{l}_{imp} \quad (19)$$

The parallel component  $\boldsymbol{\Omega}_{N\parallel}$  does not produce a moment around O and cannot be cancelled because its line of action passes through the CR. Therefore, we focus on eliminating the  $\boldsymbol{\Omega}_{N\perp}$  due to  $\mathbf{F}_{imp\perp}$ , for which

$$\mathbf{l}_{imp} \cdot \mathbf{F}_{imp\perp} = 0 \quad (20)$$

This condition corresponds to the angle requirement in (10). To zero  $\boldsymbol{\Omega}_{N\perp}$ , we require that the left side of (19) be equal to zero ( ${}^a \mathbf{l}_{imp} \neq \mathbf{0}$ ). For such a point,  ${}^a \mathbf{l}_{imp} = {}^a \mathbf{l}_{cop}$ , and therefore

$${}^a \mathbf{l}_{cop} \times (m \cdot {}^a \boldsymbol{\omega} \times {}^a \mathbf{r}_{cm}) = {}^a \mathbf{I}^o \cdot {}^a \boldsymbol{\omega} \quad (21)$$

During impact the instantaneous rotation axis is defined by

$$\hat{\mathbf{t}} = {}^a \mathbf{M} / \|{}^a \mathbf{M}\| \quad \text{with} \quad {}^a \mathbf{M} = {}^a \mathbf{l}_{imp} \times {}^a \mathbf{F}_{imp} \quad (22)$$

Let also unit vectors  $\hat{\mathbf{n}}$  and  $\hat{\mathbf{s}}$  normal to each other and to  $\hat{\mathbf{t}}$  so that an orthogonal CS  $b: \{nst\}$  is formed. The instantaneous angular velocity in this CS is then

$${}^b \boldsymbol{\omega} = \begin{pmatrix} 0 & 0 & \omega_t \end{pmatrix}^T \quad (23)$$

Equation (21) is written as

$${}^a \mathbf{I}^o \cdot {}^a \boldsymbol{\omega} = m {}^a \mathbf{r}_{cm}^\times \cdot {}^a \boldsymbol{\omega} \times {}^a \mathbf{l}_{cop} \quad (24)$$

Where  $\mathbf{r}^\times$  is the matrix that corresponds to a cross product

$$\mathbf{r} = \begin{pmatrix} x & y & z \end{pmatrix}^T \Leftrightarrow \mathbf{r}^\times = \begin{pmatrix} 0 & -z & y \\ z & 0 & -x \\ -y & x & 0 \end{pmatrix} \quad (25)$$

Eq. (24) written in frame  $b$  yields

$${}^b \mathbf{I}^o \cdot {}^b \boldsymbol{\omega} - m {}^b \mathbf{r}_{cm}^\times \cdot {}^b \boldsymbol{\omega} \times {}^b \mathbf{l}_{cop} = \mathbf{0} \quad (26)$$

Eq. (26) and (23) result in

$$\omega_t \cdot \begin{pmatrix} {}^b I_{nt}^o + m \cdot r_{cm,t} \cdot l_{cop,n} \\ {}^b I_{st}^o + m \cdot r_{cm,t} \cdot l_{cop,s} \\ {}^b I_{tt}^o - m \cdot (r_{cm,s} \cdot l_{cop,s} + r_{cm,n} \cdot l_{cop,n}) \end{pmatrix} = \mathbf{0} \quad (27)$$

where  $r_{cm,i(i=n,s,t)}$  and  $l_{cop,i(i=n,s,t)}$  refer to the  $i$  component of the corresponding vector in CS  $b$ . For (21) to be valid all three rows of (27) must be equal to zero. The case where  $\omega_t = 0$  is trivial (no impact occurs). The vector of (27) cannot be totally eliminated except if:

i)  $\hat{\mathbf{t}}$  is a principal inertia axis of the body. Then,

$${}^b I_{nt}^o = {}^b I_{st}^o = 0 \quad (28)$$

ii) There is symmetry with respect to the  $\mathbf{ns}$  plane, i.e.

$$r_{cm,j} = 0 \quad (29)$$

iii) Equation (20) applies.

iv) Using the last row of (27) and (29), the impact occurs at a point which satisfies

$${}^b \mathbf{r}_{cm} \cdot {}^b \mathbf{l}_{cop} = {}^b I_u^o \cdot m^{-1} \quad (30)$$

which by virtue of (15) and (16) it is

$${}^b \mathbf{r}_{cm} \cdot {}^b \mathbf{r}_{cop} = {}^b I_u^c \cdot m^{-1} \quad (31)$$

Eq. (31) requires that the IP, the CR and the CM should be collinear. In the planar case,  $\hat{\mathbf{t}}$  is substituted with  $\hat{\mathbf{z}}$ , and (31) reduces to (11). Also if only (20) and (31) apply, the reaction forces can be still minimized but not eliminated.

#### IV. CoP FOR MULTIBODY SYSTEMS

The CoP for multibody systems can be found using Newton-Euler Algorithm (NEA). Consider two adjacent links, Fig. 5. Note that the external impact force  $\mathbf{f}_{imp,i}$  acts on the impact point, which is located at  $\mathbf{r}_{un,i}$  from CM and  $-\mathbf{r}_{dist,i}$  from next joint  $\{i+1\}$ . To this end the equations of interest are:

$${}^i \dot{\mathbf{v}}_{C,j} = \frac{d}{dt} ({}^i \boldsymbol{\omega}_i \times {}^i \mathbf{r}_{C,j} + {}^i \mathbf{v}_i) \quad (32)$$

$${}^i \mathbf{F}_i = m_i \cdot {}^i \dot{\mathbf{v}}_{C,j} \quad (33)$$

$${}^i \mathbf{M}_i = \frac{d}{dt} ({}^{C,j} \mathbf{I}_i \cdot {}^i \boldsymbol{\omega}_i) \quad (34)$$

$${}^i \mathbf{f}_i = {}^i \mathbf{R}_{i+1} \cdot {}^{i+1} \mathbf{f}_{i+1} - {}^i \mathbf{f}_{imp,i} + {}^i \mathbf{F}_i \quad (35)$$

$${}^i \mathbf{n}_i = {}^i \mathbf{M}_i + {}^i \mathbf{R}_{i+1} \cdot {}^{i+1} \mathbf{n}_{i+1} + {}^i \mathbf{r}_{C,j} \times {}^i \mathbf{F}_i + {}^i \mathbf{r}_{i+1} \times {}^i \mathbf{R}_{i+1} \cdot {}^{i+1} \mathbf{f}_{i+1} - {}^i \mathbf{r}_{imp,i} \times {}^i \mathbf{f}_{imp,i} \quad (36)$$

Also

$${}^i \mathbf{r}_{imp,i} = {}^i \mathbf{r}_{C,j} + {}^i \mathbf{r}_{un,i} \quad (37)$$

$${}^i \mathbf{r}_{i+1} = {}^i \mathbf{r}_{C,j} + {}^i \mathbf{r}_{un,i} + {}^i \mathbf{r}_{dist,i} \quad (38)$$

where all vectors are defined in Fig. 5. Equations (32) - (36) are integrated for a small fraction of time. Algebraic elimination of a number of terms from (36) using (32) - (35) and (37) - (38) and integration of (36) yield:

$$\begin{aligned} & ({}^i \mathbf{r}_{C,j} + {}^i \mathbf{r}_{un,i}) \times {}^i \boldsymbol{\Omega}_{f,i} = \\ & \underbrace{\left[ {}^i \mathbf{r}_{un,i} \times m_i \cdot ({}^i \boldsymbol{\omega}_i \times {}^i \mathbf{r}_{C,j}) - {}^{C,j} \mathbf{I}_i \cdot {}^i \boldsymbol{\omega}_i \right]}_{\langle A \rangle} - \\ & \underbrace{\left[ {}^i \mathbf{r}_{dist,i} \times {}^i \mathbf{R}_{i+1} \cdot {}^{i+1} \boldsymbol{\Omega}_{f,i+1} \right]}_{\langle B \rangle} + \\ & \underbrace{\left[ {}^i \mathbf{r}_{un,i} \times (m_i \cdot {}^i \mathbf{v}_i) \right]}_{\langle C \rangle} + \underbrace{\left[ \int ({}^i \mathbf{n}_i - {}^i \mathbf{R}_{i+1} \cdot {}^{i+1} \mathbf{n}_{i+1}) \right]}_{\langle D \rangle} \end{aligned} \quad (39)$$

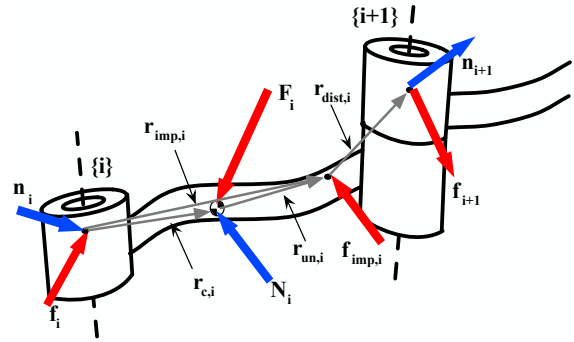


Figure 5. Free body diagram of two adjacent manipulator links.

To obtain  ${}^i \boldsymbol{\Omega}_{f,i} = 0$ , terms  $\langle A-D \rangle$  in (39) should be zero. Note that according to (20), only the normal components of a force can be eliminated. Thus for the normal components:

- $\langle A \rangle$ : is (26) so by virtue of (31)

$${}^i \mathbf{r}_{un,i} = {}^i \mathbf{r}_{cop,i} \quad (40)$$

- $\langle B \rangle$ : For this term to be zero, joint  $\{i+1\}$  must be located at the CoP of link  $\{i\}$ . To eliminate  $\langle B \rangle$  both an external impact and reaction forces from link  $\{i+1\}$  should act on this point, therefore  ${}^i \mathbf{r}_{dist,i} = 0$ . Such a case implies that the external impact force acts directly on the bearings of link  $\{i+1\}$ . For this reason, in the following analysis one force acts at a link at any time, either the impact force, or the reaction force from next link.

- $\langle C \rangle$ : is very small, since  ${}^i \mathbf{v}_i$  is small or zero and can be neglected. This is reasonable due to the assumptions set earlier.

- $\langle D \rangle$ : includes joint moments. It can be neglected due to the small time duration and the integration. However, it is expected that deviations due to the different postures of links  $\{1\}$  to  $\{i-1\}$  and links  $\{i+1\}$  to end effector, will exist.

The above analysis concludes that in order to minimize reaction forces on joint bearings, it is best to position a revolute joint at the CoP of the previous body, while the impact should occur at the CoP of the last link.

#### V. IMPLEMENTATION GUIDELINES

We focus on rotational joints as this is the most common type for space applications. It is assumed that the use of special drives, allows the links to be decoupled from their actuators, rendering the joints essentially passive. The following guidelines apply to joints, able to rotate freely:

- An impact should occur as near as possible to the measured CoP and at normal angle with respect to longitudinal axis which is defined by the RA (2D Case) or RP (3D Case) to the IP. To this end, the robotic system must prepare itself for the impact. The equations which describe the use of CoP are summarized by (20), (28), (29) and (31).

- Revolute joints should be normal to each other at the moment of the impact, see (10) and connected at their CoP, see (39) and (40)(assuming the latter property is achievable).

c. To filter an impact, in 2D systems two revolute joints are needed, while in the 3D case, three revolute joints are needed, each one for each component of the impact force.

d. In the presence of uncertainties, the configuration with successive normal links gives the best results.

e. If (d) above is not feasible, another option is to “divide” the n-body robot into two sub-bodies; the first includes bodies 1 to k-1 (body I), and the second includes bodies k to n (body II), see Fig. 6. Joint k should remain free and all the joints of body II are locked in an appropriate configuration. Calculating the impact location, the links of body II are selected so that both their characteristics and configuration can form a “rigid” body with mass and inertia according to (a) and (b). Body I rotates so that the axis of joint k will become normal to impact.

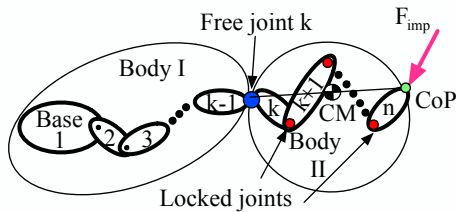


Figure 6. Proposal for exploitation of CoP for a general 3D multibody system, by locking joints in a way to create a feasible CoP.

Interesting issues related to the effect of parametric and structural uncertainties do arise. Preliminary trials show that the system response is robust to small such uncertainties.

## VI. SIMULATION RESULTS

*Planar Space Robot.* The first set of simulations refer to a planar system, Fig. 7, which consists of a thruster-equipped base, able to make x-y translational planar motions and a rotational motion around the z axis normal to its plane. Table 1 displays the physical properties of the system, including the position of CoP for the two rotational links. Simulation tests were run changing various parameters: (a) impact position on link 5, (b) the impact angle, (c) position of joint 5 on link 4 and (d) initial angles of joints  $q_1$  and  $q_2$ . Both joints are free to rotate. The impact duration is 0.01s, and the magnitude is set equal to 10kN. Note that it was more convenient to plot forces and not impulses. Also, the plots present the force components on the local coordinate frame of each joint, i.e. the normal component of the impact force is parallel to the  $y_i$  axis of the local CS of link  $i$ .

Fig. 8 presents the reaction forces at link 5 after the impact: (a) changing the point of impact, and (b) changing the angle of impact on CoP. As shown in Fig. 8a the local reaction force is almost eliminated when the impact is located in CoP, whereas in Fig. 8b, the reaction force is almost eliminated when the impact angle is normal to link 5. Deviations from zero are due to  $\langle D \rangle$  in (39). These results validate the previous analysis. Fig. 9 presents the motion of the robotic system with free joints after impact for (a) a non-ideal configuration and (b) an ideal one with the two links normal to each other, and the force acting at the CoP normal to the final link. Both simulations last for 1.2 s. At final time, the CM of base has been translated 0.22m in the first

case and 0.12m in the second case. The relatively fast link motion is due to the applied impact force and the system mass properties, which were selected for illustrative purposes. The response will be slower or faster depending on these values, but qualitatively similar.

Table 1. Physical characteristics of planar system

Link	Mass (kg)	Inertia (kg-m <sup>2</sup> )	Joint length (m)	CM (m)	CoP (m)
1	0	0	0	0	-
2	0	0	0	0	-
3	400	66.67	1	0	-
4	40	3.33	1	0.5	0.6665
5	30	2.5	1	0.5	0.6667

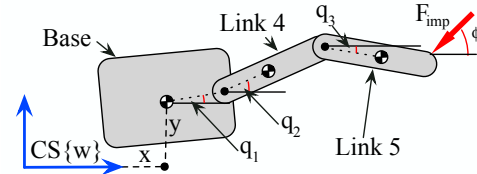


Figure 7. The 2D Space System and its dofs used in simulations.

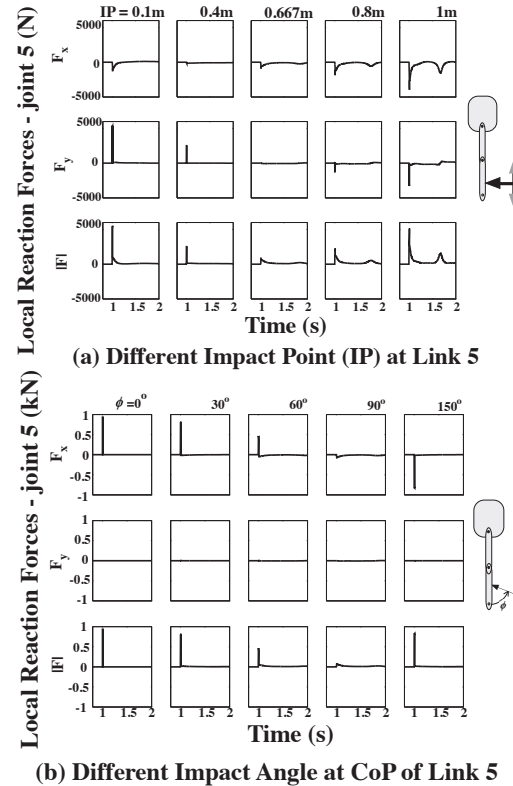


Figure 8. Reaction forces on local coordinates of joint 5 for alternating a) different impact point and b) different impact angle.

*3D 3R system.* The next set of simulations, presents a 3R PUMA-like robot with free joints. The joint axis of the first joint is at  $90^\circ$  with respect to the second one, which is parallel to that of the third joint, see Fig. 10. That is, it inherently satisfies the requirement of guideline (a). The properties of the system are presented in Table 2. The manipulator can be fixed on a large base, e.g. ISS or the Earth. The reaction forces on the bearings of joints and the reaction on the base are of interest. The impact force is  $\mathbf{F}_{imp} = [1 \ 1]^T$  kN,  $\|\mathbf{F}_{imp}\| = 1.732$  kN, with duration 0.01s.

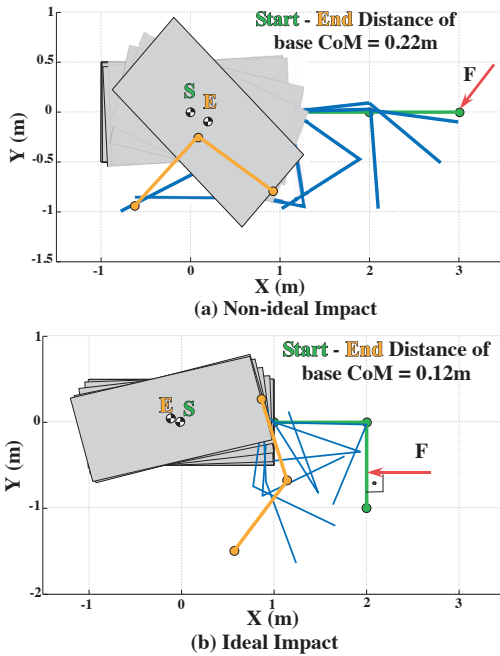


Figure 9. Motion snapshots of the 2D system with free joints following impact. (a) non-ideal configuration, (b) ideal configuration.

Fig. 11 presents the results for two different setups; the blue dotted line presents a configuration, where all joints are located at CoP of links (denoted by C,C,C) and the initial angles are  $(q_1, q_2, q_3) = (0^\circ, 0^\circ, 90^\circ)$ . The red solid line presents a random setup with joints at the tip of each link (denoted by 1,1,1) and initial angles  $(q_1, q_2, q_3) = (0^\circ, 30^\circ, 45^\circ)$ .

Table 2. Properties of RRR system under evaluation.

Link	Mass (kg)	Inertia (kg-m <sup>2</sup> )	Joint length (m)	CM (m)	CoP (m)
1	10	1	1	0.2	0.5
2	20	2.5	1	0.3	0.417
3	5	0.5	1	0.15	0.667

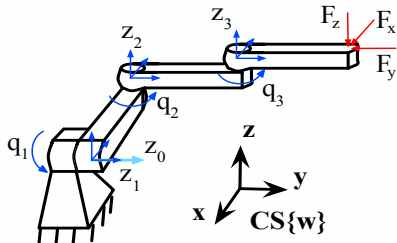


Figure 10. The 3D RRR robotic system under evaluation.

Table 3 presents the magnitude of reaction forces per joint for some characteristic configurations and impact points or joint positions. As both the Fig. 11 and Table 3 show, the use of CoP has advantages. In Fig. 11 one may observe that at joint 1 (base) the forces developed are much lower when the guidelines are satisfied. However they are not zero due to the dynamic coupling between links and joints 1 and 2, and due to  $\langle D \rangle$  in (39). This can be seen also in the third and fourth cases of Table 3, where the third link has the same setup (impact on CoP) but different magnitudes have been found. Still the configuration with normal links and impacts on CoP minimizes the impulse reactions at the base.

Table 3. Max reaction forces as a function of configuration & joint location.

Absolute Forces in N	1 <sup>st</sup> Case (0°, 0°, 0°) (1, 1, 1)	2 <sup>nd</sup> Case (0°, 0°, 0°) (1, C, C)	3 <sup>rd</sup> Case (0°, 0°, 90°) (1, 1, C)	4 <sup>th</sup> Case (0°, 0°, 90°) (C, C, C)
Joint 1	1583	1390	419	310
Joint 2	1520	1337	355	220
Joint 3	1307	1260	838	997

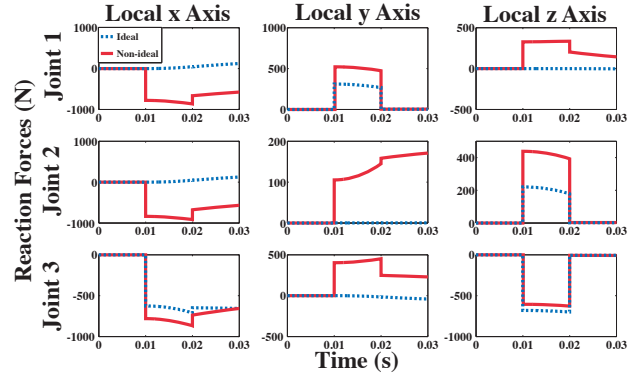


Figure 11. Reaction forces at the RRR for two distinct configuration cases.

## VII. CONCLUSIONS

This work examined the use of the CoP during impacts. It has been shown that for any multibody system, there are advantages using the CoP. By following particular strategies prior to impact, the reaction forces on joints can be effectively minimized. Simulations validated this proposition. Implementation guidelines that make use of the CoP advantages for manipulators have been presented. The analysis was developed with space robots in mind; however this analysis can be utilized also by other robotic systems.

## VIII. REFERENCES

- [1] Papadopoulos, E. G., and Moosavian, S. A. A., "Dynamics & Control of Multi-arm Space Robots During Chase & Capture Operations," *Int. Conf. on Intelligent Robots and Systems*, pp. 1554-1561, Munich, Germany, 1994.
- [2] Yoshida, K., and Sashida, N., "Modeling of Impact Dynamics and Impulse Minimization for Space Robots," *Int. Conf. on Intelligent Robots and Systems*, pp. 2064-2069, Yokohama, Japan, 1993.
- [3] Yoshida, K., and Nakanishi, H., "Impedance Matching in Capturing a Satellite by a Space Robot," *Int. Conf. on Intelligent Robots and Systems*, pp. 3059-3064, Las Vegas, Nevada, 2003.
- [4] Dimitrov, D. N., and Yoshida, K., "Momentum distribution in a space manipulator for facilitating the post-impact control," *Int. Conf. on Intelligent Robots and Systems*, pp.3345-3350, Sendai, Japan, 2004.
- [5] Cross, R., "Center of percussion of hand-held implements," *American Journal of Physics*, vol. 72(5), pp. 622-630, 2004.
- [6] Alba, M. et al., "Center of percussion and gait design of biped robots," *Mechanism and Machine Theory*, vol. 45(11), pp. 1681-1693. Elsevier, 2010.
- [7] Arisumi, H. et al, "Dynamic Lifting Motion of Humanoid Robots," *Int. Conf. Robotics & Automation*, pp. 2661-2667, Rome, Italy, 2007.
- [8] Ioi, K. et al, "Mechanical and control design of caster for low vibrations and crashes of carts," *Int. Conf. on Mechatronics and Automation*, pp. 1688-1693, Beijing, China, 2011.
- [9] Svinin, M.; Kaneko, M.; Yamamoto, M.; , "On the percussion center of flexible links," *IEEE Int. Conf. on Robotics and Automation (ICRA)*, pp.330-335, Shangai, China, 2011.
- [10] Papadopoulos, E. G., and Paraskevas, I. S., "Design and Configuration Control of Space Robots Undergoing Impact," *6th Int. ESA Con. on GNC*, Loutraki, Greece, 2005.
- [11] Stronge, W. J., "Impact Mechanics", Cambridge Univ. Press, 2000.